

## 論文内容の要旨

### 論文題目 **Kinetics of isotopic fractionation and diffusion of magnesium induced by evaporation of forsterite**

(フォルステライトの蒸発に伴うマグネシウムの同位体分別及び拡散のカイネティクス)

氏名 山田 真保

Evaporation of solid materials under low-pressure and high-temperature conditions would have played important roles in chemical and isotopic fractionations in the early solar system recorded in planetary materials. Forsterite ( $\text{Mg}_2\text{SiO}_4$ ) consists of major rock-forming elements (Mg, Si and O) and is thus one of the major minerals in the earth, meteorites, planets and interstellar space. It is therefore important to understand the kinetic aspect of evaporation of forsterite to understand the time scale of evolution of condensed phases in the early solar system.

Forsterite evaporates congruently both in equilibrium and under kinetic conditions. The evaporation behavior of forsterite, such as an evaporation rate and its dependence on temperature and hydrogen pressure, has been experimentally investigated in vacuum and in hydrogen (e.g., Hashimoto, 1990; Nagahara and Ozawa, 1996).

Kinetic evaporation leads to enrichment of heavier isotopes in the evaporation residue due to preferential evaporation of lighter isotopes. Fractionation of Mg isotopes due to evaporation of forsterite has been investigated by Wang et al. (1999): the heavier isotope enrichment at the evaporating surface propagated into the interior of the evaporation residue due to diffusion. Wang et al. (1999) applied a diffusion-controlled isotopic fractionation model to isotopic zoning profiles and obtained the isotopic fractionation factor for evaporation of Mg and the self-diffusion coefficient of Mg in forsterite along the a-axis of forsterite. Because such a diffusion-limited isotopic fractionation during evaporation of a solid is a consequence of two thermally activated processes, diffusion and evaporation, it can potentially put strong constraints on thermal histories of planetary materials.

Anisotropy of kinetic processes may provide another important information to constrain the history of crystals such as isolated forsterite grains in chondrites. The anisotropy in the evaporation rate and microstructure of a surface of residual forsterite has been found (Ozawa et al., 1996), and it is thus expected that the isotopic fractionation factor for evaporation of Mg from forsterite is also anisotropic.

In this thesis, I measured isotopic compositions of forsterite, evaporated in vacuum along different crystallographic axes by depth profiling with ion microprobe in order to investigate anisotropy of isotopic fractionation and to determine the self-diffusion coefficient of Mg and the isotopic fractionation factor for evaporation of Mg from forsterite. I focused on the anisotropy of the kinetic parameters, which is an essentially important feature of crystals but has not yet been investigated in detail.

Evaporation experiments of single crystals of forsterite, which were cut into rectangular parallelepipeds along three crystallographic orientations, were carried out in a vacuum furnace. The samples were heated at 1500-1700°C for 12-166 hours, and the evaporation rates were obtained by weight loss. The obtained evaporation rates were fastest along the c-axis and slowest along the b-axis, which is consistent with Ozawa et al. (1996).

Magnesium isotopic compositions of evaporated forsterite were measured by an ion microprobe, CAMECA ims-6f at Department of Earth and Planetary Science in the University of Tokyo. A primary beam of  $^{16}\text{O}^-$  with an accelerating voltage of 12.5 kV and intensity of 10-40 nA was scanned over an area of  $150\mu\text{m} \times 150\mu\text{m}$ . Secondary ions of  $^{24}\text{Mg}^+$ ,  $^{25}\text{Mg}^+$ , and  $^{26}\text{Mg}^+$  were collected from the central flat part ( $50\mu\text{m} \times 50\mu\text{m}$ ) of the scanned area using digital and mechanical apertures and were counted for 0.7, 5, and 5 sec, respectively, on the electron multiplier at a mass resolving power of  $\sim 4000$ . The mass resolving power of 4000 was sufficient to avoid the interference of  $^{24}\text{MgH}$  to  $^{25}\text{Mg}$ . The offset voltage of -120 V was applied to the accelerating voltage of secondary ions to minimize the effect of the change of depth on the instrumental mass fractionation and to make the interference of  $^{24}\text{MgH}$  to  $^{25}\text{Mg}$  negligibly small. The magnesium isotopic composition of the starting material was also measured as a reference.

The evaporated samples showed positive  $\delta^{25}\text{Mg}$  and  $\delta^{26}\text{Mg}$  that are expressed as deviations from  $^{25}\text{Mg}/^{24}\text{Mg}$  and  $^{26}\text{Mg}/^{24}\text{Mg}$  ratios in a starting forsterite, and heavier isotopes are most enriched near the evaporated surface along all the crystallographic directions (Fig.1). The degree of isotopic fractionation of  $^{26}\text{Mg}$  was twice as large as  $^{25}\text{Mg}$ , indicating mass-dependent isotopic fractionation. The degree of enrichment of heavier isotopes becomes smaller with depth, and the isotopic composition approaches to that of the starting material (Fig.1). The depth profiles along the a-, b-, and c-axes of forsterite evaporated under the same conditions show clear anisotropy in isotopic fractionation profiles in terms of both the slope of the profile and the degree of fractionation at the surface (Fig.1). The difference in depth profiles of isotopic composition along different crystallographic orientations reflects anisotropy both in the isotopic fractionation at the surface by evaporation and in diffusion within the residue.

The magnesium isotopic zoning profiles were explained by the diffusion-controlled isotopic fractionation model (Wang et al., 1999), which allowed us to obtain a self-diffusion coefficient of magnesium ( $D$ ) and an isotopic fractionation factor for evaporation of magnesium ( $\alpha$ ) along the a-, b-, and c-axes in the temperature range of  $\sim 1500$ -1700°C.

The diffusion coefficient shows anisotropy, where  $D$  is largest along the c-axis and smallest along the

a-axis (Fig. 2). The activation energy for diffusion at 1500-1700°C ranges from ~550 to ~640 kJ/mol. The activation energies along the three crystallographic axes are consistent with that along the a-axis in the same temperature range (608 kJ/mol; Wang et al., 1999), whereas they are higher than those obtained in previous studies at lower temperatures (~300-480 kJ/mol; Morioka, 1981; Andersson et al., 1989; Chakraborty et al., 1994). This suggests that diffusion of Mg at 1500-1700°C occurred in the intrinsic diffusion regime, where thermally generated cation vacancies in M1 sites would be dominant, and that the enthalpy of formation of M1 vacancy is ~70-340 kJ/mol. The estimated formation enthalpy for the M1 vacancy seems to be consistent with that obtained theoretically (Lasaga, 1980; Walker, 2004).

The isotopic fractionation factor for kinetic evaporation ( $\alpha$ ) has been theoretically predicted to be expressed by square root of the inverse mass ratio of evaporating gas species containing different isotopes, i.e.,  $(i/24)^{1/2}$  ( $i=25$  or  $26$ ). Although predicted  $\alpha$  should be constant irrespective of crystallographic orientations and temperature, I found that  $\alpha^i$  has clear dependence on crystallographic orientations and weak dependence on temperature (Fig. 3 for  $\alpha^{26}$ ). The  $\alpha^{25}$  and  $\alpha^{26}$  seem to be larger along the c- and a-axes than along the b-axis, respectively, especially at higher temperatures. Another important feature of  $\alpha^i$  is that it is not as large as  $(i/24)^{1/2}$  along all the crystallographic orientations. The isotopic fractionation factor closer to unity than expected has been reported for Mg from forsterite along the a-axis (Wang et al., 1999), for Mg and Si from CAI-like silicate melts (e.g., Wang et al., 2001), and for Mg, Si, and O from forsterite melt (Davis et al., 1990).

I propose that the isotopic fractionation factor for evaporation can be expressed by the ratio between detachment rates of isotopes, which depend on vibrational frequencies between an adatom and a surface atom (or atomic cluster). If the vibration mode with a maximum frequency is responsible for detachment of adatoms, the isotopic fractionation factor is then expressed by the inverse ratio of reduced mass of the vibrating system. When an Mg atom vibrates with a surface O atom or a SiO<sub>4</sub> tetrahedral cluster,  $\alpha^{26}$  can be 1.015 and 1.032, respectively, which seem to correspond to the range of the  $\alpha^{26}$  obtained in this study. The weak temperature dependence of  $\alpha^i$  may be explained by the change of the surface atom (or atomic cluster) vibrating with Mg from a SiO<sub>4</sub> tetrahedron at higher temperatures to O at lower temperatures. Anisotropy may also be explained by the difference of the surface atom (or atomic cluster) vibrating with Mg: the surface O atom may be the dominant component vibrating with Mg at the (010) surface with the largest bond density. This mechanism could also work for isotopic fractionation during evaporation of silicate melts.

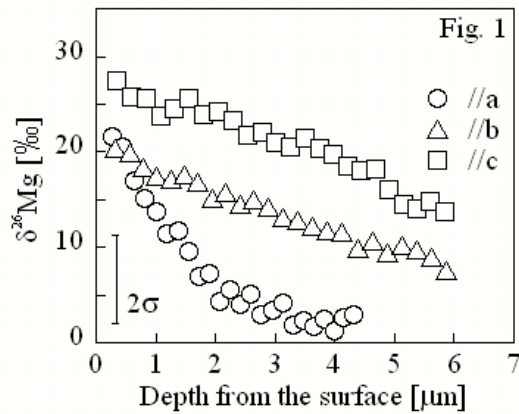


**Fig. 1:** Depth profiles of Mg isotopic compositions ( $\delta^{26}\text{Mg}$ ) along three crystallographic axes of forsterite evaporated at  $1700^\circ\text{C}$  for 6 hours.  $\delta^{26}\text{Mg}$  is expressed by  $((^{26}\text{Mg}/^{24}\text{Mg})_{\text{sample}}/(^{26}\text{Mg}/^{24}\text{Mg})_{\text{starting material}} - 1) \times 1000$  (‰). A typical  $2\sigma$  error that includes uncertainties of isotopic measurements of both an evaporation residue and a starting material is also shown.

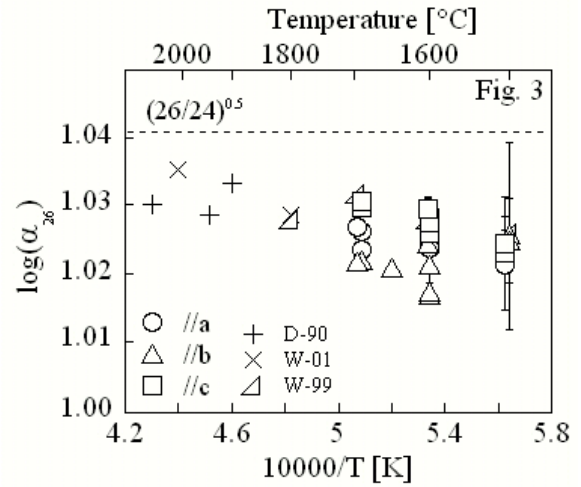


**Fig. 3:** Isotopic fractionation factor of  $^{26}\text{Mg}$  for evaporation along three crystallographic axes of forsterite. D-90:  $\alpha_{26}$  for a forsterite melt (Davis et al., 1990). W-99:  $\alpha_{26}$  along the a-axis of forsterite (Wang et al., 1999). W-01:  $\alpha_{26}$  for a chondritic silicate melt (Wang et al., 2001).

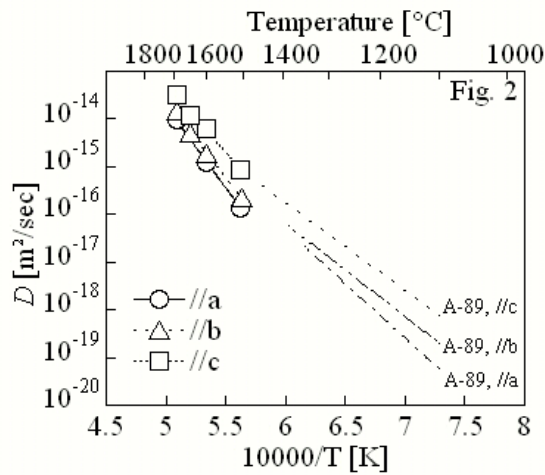


**Fig. 2:** Self-diffusion coefficients of Mg along three crystallographic axes of forsterite in the temperature range of  $1500\text{--}1700^\circ\text{C}$ . A-89: Andersson et al. (1989).